EXPERIMENTAL MODELS AND INSTRUMENTAL SURVEYS FOR RISK ASSESSMENT IN HYGIENE AND EPIDEMIOLOGY

UDC 615.9, 614.7
DOI: 10.21668/health.risk/2016.4.10.eng

IMPACT OF SILICA DIOXIDE NANOPARTICLES ON THE MORPHOLOGY OF INTERNAL ORGANS IN RATS BY ORAL SUPPLEMENTATION

N.V. Zaitseva[1], M.A. Zemlyanova[1,2,4], V.N. Zvezdin[1,4], A.A. Dovbysh[1], I.V. Gmoshinskiy[3], S.A. Khotimchenko[3]

[1]Federal Scientific Center for Medical and Preventive Health Risk Management Technologies, 82 Monastyrskaya Str., Perm, 614045, Russian Federation
[2]Perm National Research Polytechnic University, 29 Komsomolskiy Ave., Perm, 614990, Russian Federation
[3]Federal research centre of nutrition and biotechnology, 2/14 Ustinskiy Proezd, Moscow, 109240, Russian Federation
[4]Perm State National Research University, 15 Bukireva Str., Perm, 614990, Russian Federation

The object of the study was amorphous silica dioxide (SiO_2), which is widely used as a food additive (E551), a subsidiary component in pharmaceutical preparations, perfumery and cosmetic products etc. In the specification of JECFA silica dioxide does not have information about the size of its particles, which allows the use of fine amorphous SiO_2, obtained by gas phase hydrolysis of tetrachlorosilane as a food additive. This material, known as the "Aerosil", is characterized by the size of the specific surface area of 300–380 m^2/g and the size of its relatively weakly agglomerated particles of 6–30 nm, i.e., it is a nanomaterial. In the biological model the morphological changes in organs and tissue systems on oral supplementation of nanoscale particles of silica dioxide were studied. Wistar male rats were given nanosized silica dioxide with specific surface area of 300 m^2/g and primary nanoparticle size on the basis of data of electrical, atomic-powered microscopy, and dynamic light scattering in the range of 20–60 nm during 92 days. Light microscopic morphological examination of organs of rats showed a relatively mild inflammation in the structure of parenchymal organs (liver, kidney), not showing a certain dose-dependent nanoparticles. The most pronounced changes were in ileum morphology, consisting of a massive lymph macrophage and eosinophil infiltration of villi, without any apparent violation of their epithelial layer structure, which indirectly indicates the absence of violations of the barrier function of the intestinal epithelium. At the maximum dose of 100 mg/kg bw, the increased immune response was the most significant in the wall of the ileum. The results indicate the potential risks to human

Nina V. Zaitseva – Member of RAS, Doctor of Medical Sciences, Professor, Director (e-mail: znv@fcrisk.ru; tel.: +7 (342) 233-11-25).

Marina A. Zemlyanova – Doctor of Medical Sciences, Professor, head of the department of biochemical and cytogenetic diagnostic methods, Professor of Human Ecology and Life Safety (e-mail: zem@fcrisk.ru; tel.: +7 (342) 236-39-30).

Vasiliy N. Zvezdin – PhD, Head of the Health Department of Children and Adolescents (e-mail: zvezdin@fcrisk.ru; tel.: +7 (342) 237-25-34).

Anastasiya A. Dovbysh – Laboratory toxicologist metabolism and pharmacokinetics (e-mail: dovnastja@yandex.ru; tel.: +7 (342) 236-39-30).

Ivan V. Gmoshinskiy – Doctor of Biological Sciences, leading researcher of the Laboratory of Food Toxicology and Nanotechnology safety assessment (e-mail: gmosh@ion.ru; tel.: +7 (495) 698-53-71).

Sergey A. Khotimchenko – MD, Professor, Head of Laboratory of food toxicology and safety assessment of nanotechnology, Acting Deputy Director for Science, (e-mail: hotimchenko@ion.ru; tel.: +7 (495) 698-52-35).

health when using SiO_2 having a specific surface area of 300 m^2/g or higher in the composition of food products as a food additive.

***Key words**: nanoparticles, silica dioxide, morphological studies, oral supplementation, subacute toxicity, health risks.*

Amorphous silicon dioxide (SiO2) is widely used as a food additive (E551) as well as accessory ingredient in pharmaceuticals, perfumes and cosmetics. JFCFA specification dedicated to silicon dioxide [25] doesn't contain any information on its particles' size and it allows using superfine amorphous SiO2, obtained via gas-phase hydrolysis of tetrachlorsilane, as a food additive. This material well-known as "Aerosil" has specific surface area equal to 300-380 m2/g, and its relatively feebly agglomerated particles are 6-30 nm in size so we can name it a nanomaterial (NM).

The necessity to assess NM safety and health risks is justified in Resolution issued by Chief Sanitary Inspector of the RF No. 54 dated July 23, 2007 "On surveillance over products obtained via nanotechnologies and containing nanomaterials" and Rospotrebnadzor information letter "On surveillance over manufacturing and turnover of products containing nanomaterials" [2, 6].

Preliminary assessment of a degree at which silicon dioxide nanoparticles may be hazardous according to the existing Methodical Guidelines 1.2.2522-09 implies at moderate potential hazard of this nanomaterial. This fact requires a profound toxicological and hygienic study of this material in tests in vivo using laboratory animals and applying a whole set of integral, morphological, biochemical and other toxicity markers.

The purpose of this work was to study the influence exerted by nano-sized SiO2 on morphology of rats' internal organs at oral introduction during 92 days.

Data and methods. We used high-disperse amorphous SiO2 obtained from "Silika" LLC (Dolgoprudniy city, Moscow region, Russia) in our work; the material is sold under commercial name "Orisil 300" and corresponds to State Standard 14922-77. It is light white powder which, under dispersing with ultrasound in water, turns into opalescent colorless colloidal solution; the solution remains stable for not less than 2 days. Specific surface area of the product, detected via technique of inert gases adsorption isotherms, amounted to 300 m2/g as per the manufacturer's data. Specialists at "Scientific Research Institute for Nutrition" and "Biochemistry Institute named after A.N. Bach" accomplished some studies of the nanomaterial using transmission electron microscopy techniques, atomic-force microscopy and dynamic light scattering [8]. The characteristics drawn by them revealed (Figure 1), that a dry product contains mostly primary particles agglomerates sized from 5 to 100 nanometers. Analysis of particles size distribution in ultrasound-treated water suspension in 1% concentration as per mass showed that the prevailing nanoparticles fraction had average numeric hydrodynamic diameter equal to 6.6±32.1 nanometers, 90-th size percentile was 91.7 nanometers. At the same time a share of particles with diameter exceeding 100 nanometers was below 10% of the total particles number.

All the work with animals was performed in conformity with The Guide for the Care and Use of Laboratory Animals (ILAR, DELS) and Laboratory Practice Rules [5, 16]. The research was accomplished in accordance with guidelines on nanomaterials safety assessment [4]. The experiment was performed on 75 Wistar male rats with initial body weight equal to 80 grams obtained from "Stolbovaya" nursery. The animals received balanced semi-synthetic nutrition during the whole experiment. They were placed in cages, 3 animals in each, and had free unlimited access to food and water. At the beginning of the experiment the rats were randomly divided into 5 groups with the same quantity of animals (15) in each, the only condition being analogical initial average body weight. We

introduced a carrier (deionized water) into animals from the 1st (control) group. Rats from groups 2, 3, 4 and 5 received nano-sized SiO2 in the form of ultrasound-treated suspension in deionized water (treatment period was 5 minutes, frequency equal to 44 kHz, power being 1 W/cm3). During the first 30 days the nanomaterial was introduced via gastric tube; later on SiO2 suspension was added to the animals' food for the following 62 days; the dose was calculated basing on the quantity of food eaten. Introduced SiO2 dose in groups 2, 3, 4 and 5 amounted to 0.1, 1.0, 10 and 100 mg/kg of body weight correspondingly. On the 93th day the animals were taken out of the experiment via dehematizing from postcava under ether anesthesia. The selected samples of internal organs (liver, kidneys, and ileum) were instantly placed into fixing fluid (3.7% formaldehyde solution in 0.1M sodium-phosphate poiser pH 7.00±0.05) and transported to the laboratory for further examination.

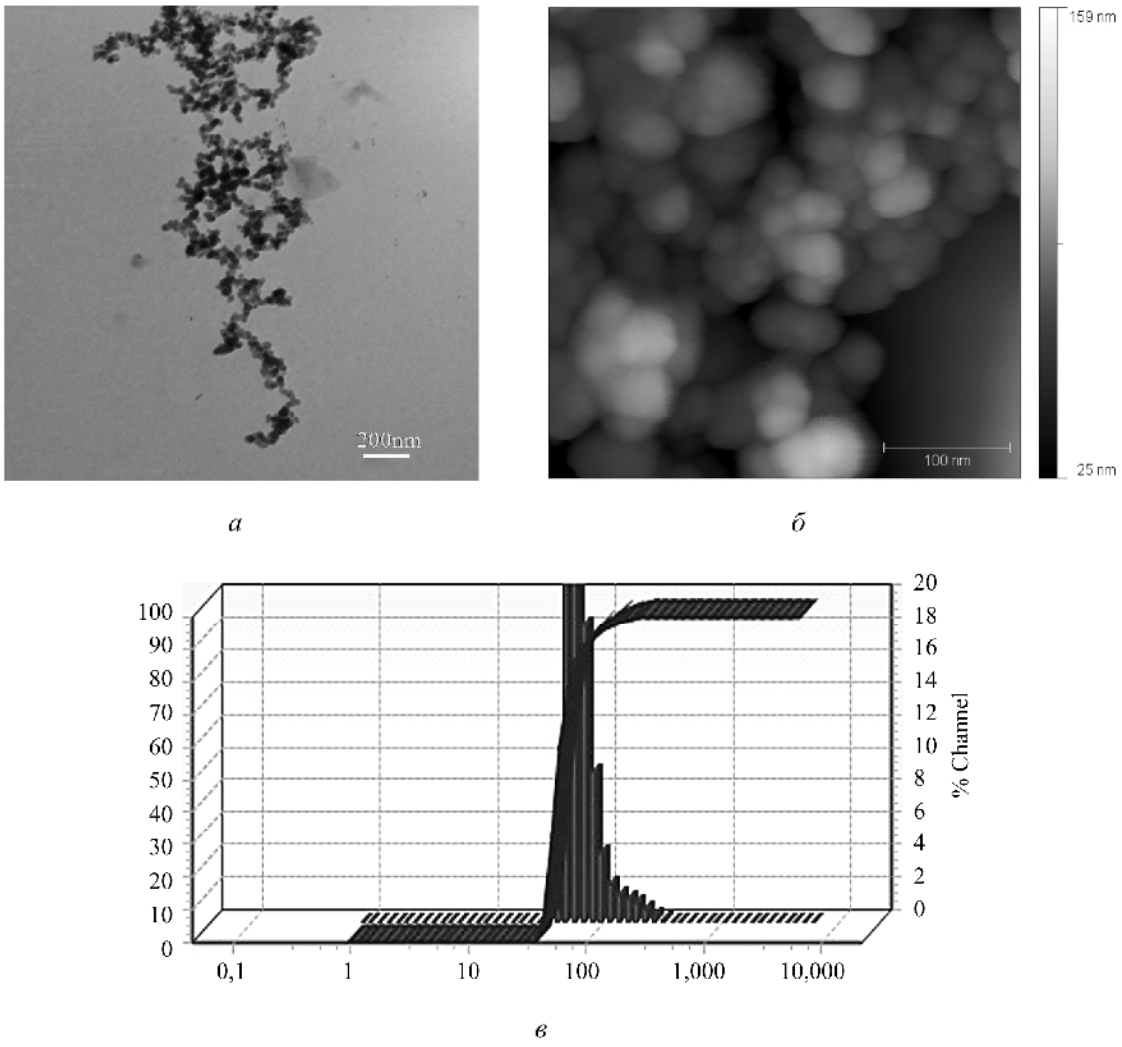

Figure. 1. Amorphous silicon dioxide "Orisil-300" particles size: a) is obtained via electronic microscopy (JEM-100CX microscope, JEOL, Japan), sample microscopy without ultrasound treatment; б) is obtained via atomic-force microscopy (SmartSPM microscope, AIST-NT, Russia), sample microscopy without ultrasound treatment; в) is obtained via dynamic light scattering technique (Nanotrack Wave device, Microtrack Inc., USA), distribution as per particles size of a sample treated with sound. Taken from work [5] with the authors' consent.

Histological specimens preparation included organs' parts dehydration in alcohols with ascending concentration, impregnation with chloroform and paraffin in «Excelsior ES» automatic histological processor (Thermo Scientific, Germany). Then the samples were embedded in homogenized paraffin medium «Histomix» [1] at «Histo Star» block embedding station (Thermo Scientific, Germany). Paraffin sections with 3-4 μm width were made with the use of «JUNG SM 2000R» sliding microtome (Leica, Germany) and then painted as per conventional technique [3] with hematoxylin and eosin in «Varistain Gemini ES» panting robot (Thermo Scientific, Germany). The obtained microslides were studied with the use of «MEI-JI» light optical microscope (Techno, Japan) at magnification equal to ×50, ×100, ×200, ×400, ×800, ×1000. Microphotos were made with «Microscopy VISION» camera (VISION, Canada). Not less than 9 microslides were made out of each organ. The total number of analyzed microslides (sections) of organs amounted to 400.

Results and discussion. The results of internal organs examination performed on all the animals from group 1 (control group) revealed that there was persistent hyperplasia of ileum lymphoid tissue with secondary follicles formation. Feebly apparent lymphoid infiltration and solitary eosinophils were detected in hepatoportal tracts in some microslides. No visible morphologic changes were detected in the animals' kidneys. On the whole, morphological state of internal organs taken out of the rats from control group corresponded to the physiological standard for animals of such sex and age.

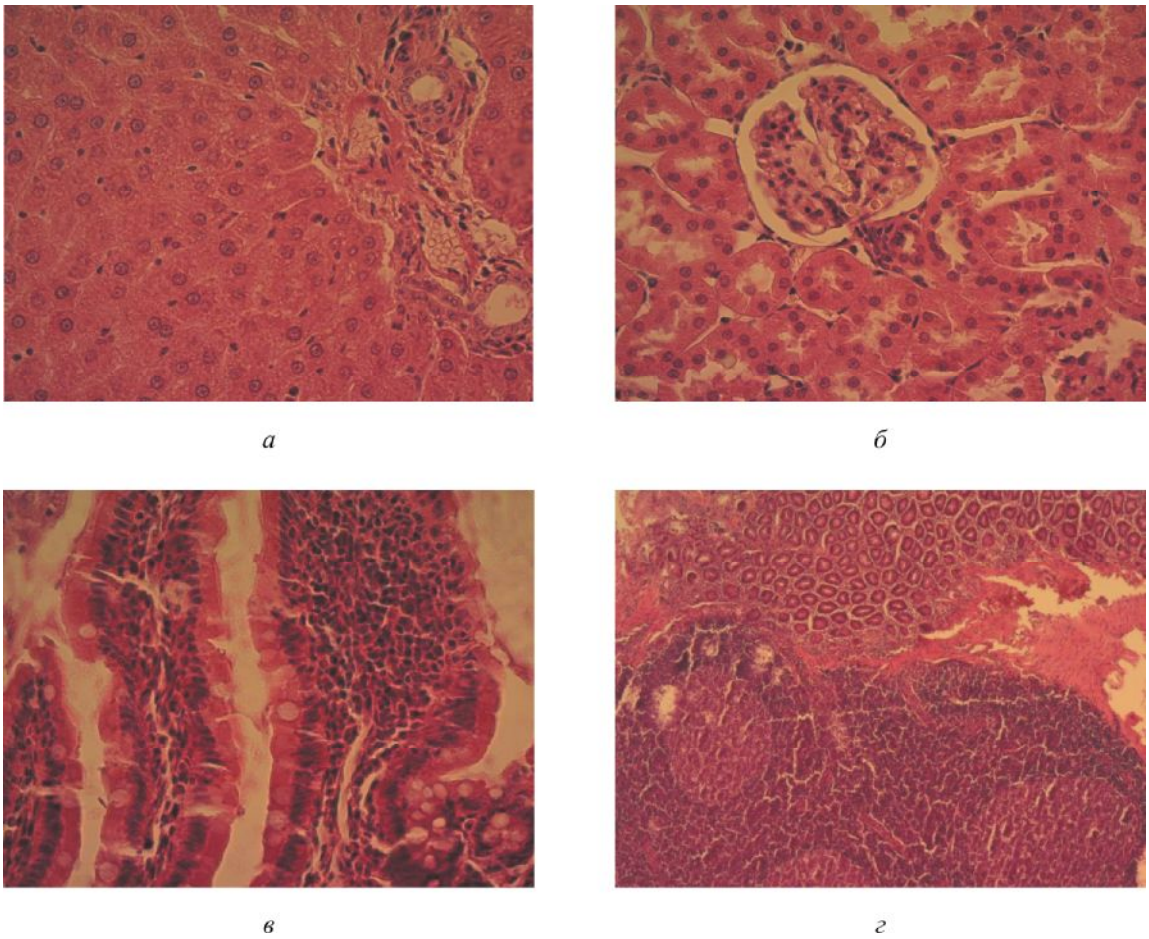

Figure 2. Representative microphotos of a rat from group 1 (control) (painted with hematoxylin and eosin), magnification ×200 (а, г), ×400 (б, в): *а* is liver, б is kidneys; *в, г* is ileum

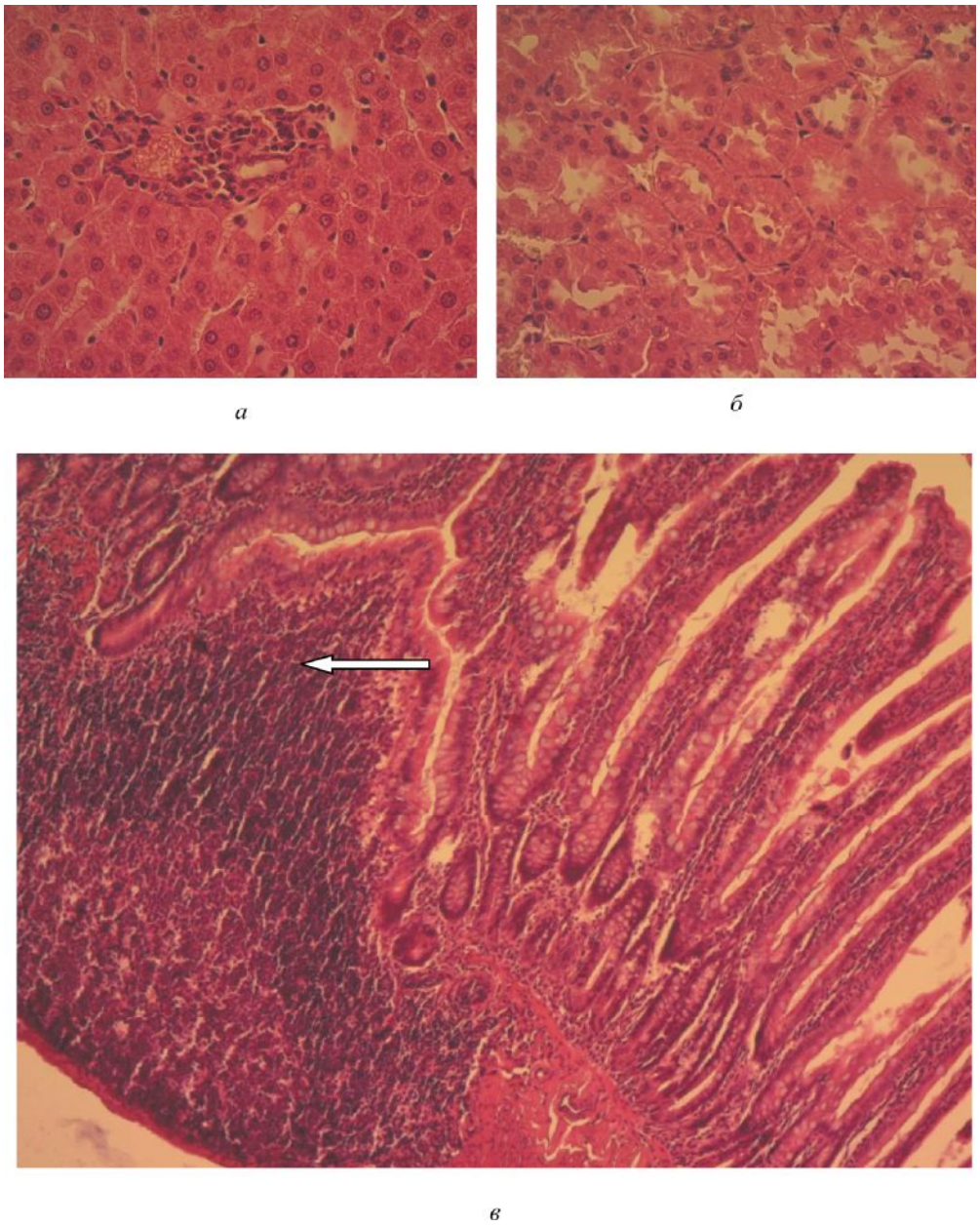

Figure 3. Representative microphotos of a rat from group 2 (silicon dioxide, 0,1 mg/kg b.w.) (painted with hematoxylin and eosin), magnification ×200 (а, б); ×400 (в): а is liver; б is kidneys; в is ileum. Arrow points at internodule lymphoid tissue.

Representative microphotos of liver, kidney and ileum section of the rats from control group are shown in Figure 2.

Animals from group 2 (silicon dioxide dose equal to 0.1 mg/kg of body weight) had feebly apparent focal dust-like and atomized lipid parenchymatous degeneration and eosinophilia of portal tracts infiltrate in their liver (Figure 3a).

Feebly apparent mesangial cells proliferation was detected in some glomerules (up to 6 in a lobule) without any increase in mesangial matrix volume; there was also focal swelling of cells in external leaf of nephron capsule (Figure 3b). We detected large trapezoidal cells with considerable eosinophilic granules in apical part and dark nucleus in basal sections - Paneth cells - in the base of ileum mucous tunic crypts. Solitary lymph nodes were large with big reactive centers and wide cellular mantle zones; they penetrated into submucous layers from proper layer. Peyer's plaques

came from proper layer of mucous tunic into submucous layer. Bowel lumen was greatly narrowed in the zones where large Peyer's plaques were located. Lymph nodes between villi evaginated mucous tunic into bowel lumen in a form of a cupula which was covered with low epithelial cells with a great quantity of lymphocytes and macrophages (Figure 3c). There was a slight edema, moderate infiltration from eosinophils, macrophages, lymphocytes and plasma cells, in submucous layer.

Liver hepatocytes in animals from group 3 (silicon dioxide dose equal to 1 mg/kg of b.w.) were in the state of focal dust-like and atomized lipid degeneration; there were numerous small transparent drops with sharp contours in cells cytoplasm and some hepatocytes with two nucleuses were detected. We observed infiltration of lymphocytes, macrophages, and plasma cells with solitary eosinophils admixture in portal tracts and sinusoids (Figure 4a).

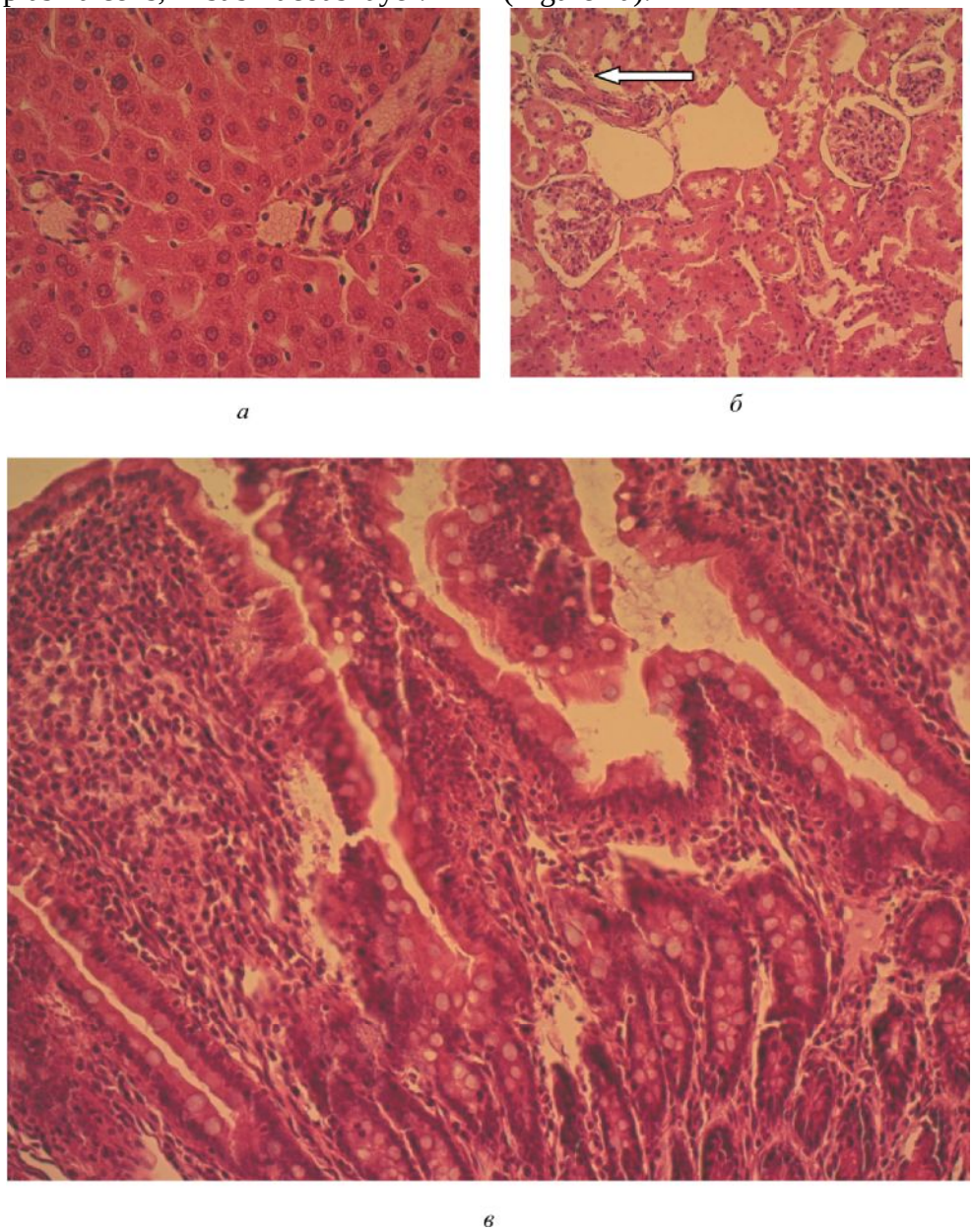

Figure 4. Representative microphotos of a rat from group 3 (silicon dioxide, 1.0 mg/kg b.w.) (painted with hematoxylin and eosin), magnification ×200 (а, б); ×400 (в): a is liver; б is kidneys, arrow points at a vein; в is ileum.

There were no signs of mesangial cells proliferation and proliferation of capsule external leaf cells in kidneys of animals from this group. Just a slight number of glomerules had focal swelling of capsule external leaf cells (Figure4b).

Villi in ileum mucous tunic were of various form and width due to uneven edema and cellular infiltration from lymphocytes, macrophages, and numerous eosinophils (Figure 4c).

Bunches of lymphocytes, macrophages, plasma cells, and numerous eosinophils occurred in proper layer. There were large bunches of Paneth cells in the base of crypts. Solitary follicles and Peyer's plaques follicles were large with big reactive centers and wide mantle zones converting into internodal lymphoid tissue. Follicles from mucous layer penetrated into submucous layer and made muscular tunic substantially thinner. Crypts in Peyer's plaques view were not deep or they were even absent; villi were short and irregular-shaped.

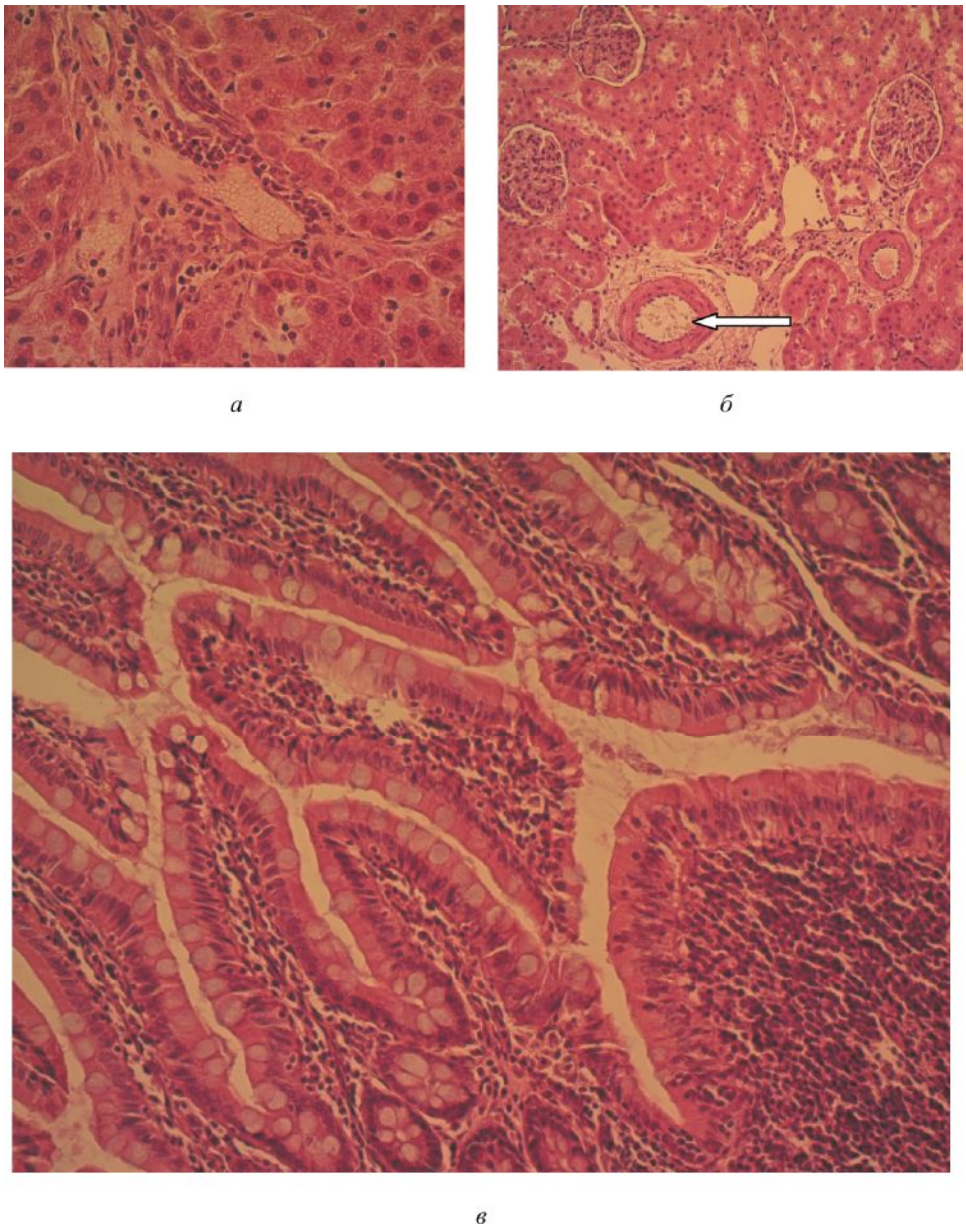

а *б* *в*

Figure 5. Representative microphotos of a rat from group 4 (silicon dioxide, 10 mg/kg b.w.) (painted with hematoxylin and eosin), magnification ×200 (а, б); ×400 (в): а is liver; б is kidneys, arrow points at an artery; в is ileum, arrow points at Paneth cells.

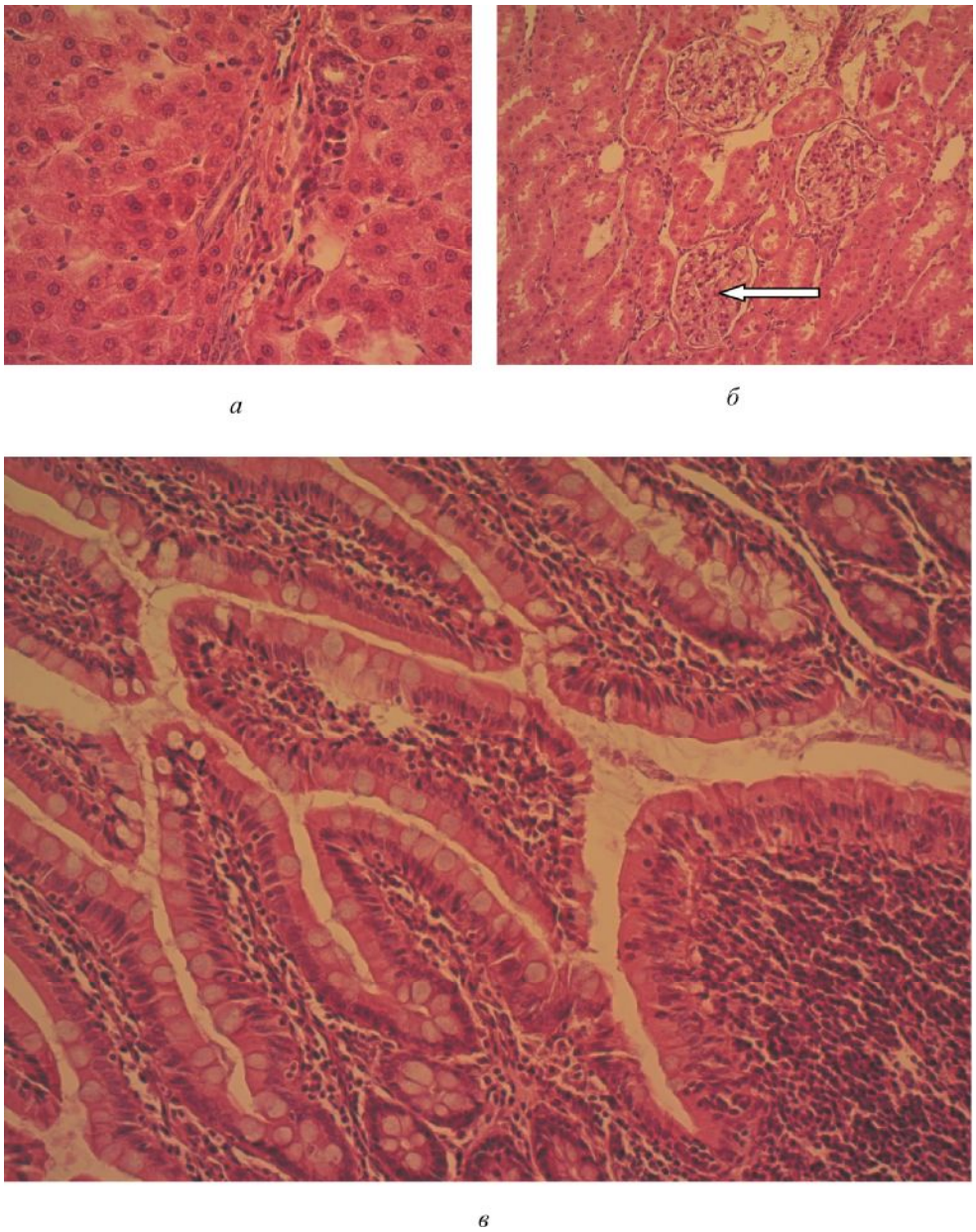

Figure 6. Representative microphotos of a rat from group 5 (silicon dioxide, 100 mg/kg b.w.) (painted with hematoxylin and eosin, magnification) ×200 (а, б); ×400 (в): а is liver; б is kidneys, arrow points at an artery; в is ileum

Lymphoid nodes formed mucous tunic evaginations between villi in a form of cupula covered with low epithelial cells with a great number of lymphocytes and macrophages. There were bunches of lymphocytes, macrophages, plasma cells, and numerous eosinophils in submucous layer.

Liver hepatocytes in animals from group 4 (silicon dioxide dose equal to 10 mg/kg of b.w.) had polygonal form, one or two nucleuses with fine-dispersed chromatin condensed at nuclear membrane and apparent nucleoluses. Hepatocytes cytoplasm was granular (Figure 5a).

Portal tracts contained evident infiltration from eosinophils, macrophages, lymphocytes, and plasma cells; some infiltrate cells penetrated into periportal sinusoids. We observed feebly apparent mesangial cells proliferation in glomerules (up to 6 in a lobule) without any increase in mesangial matrix volume (Figure 5b). There were no signs of proliferation of

capsule external leaf cells. A slight edema occurred in proper layer of ileum mucous tunic together with moderate lymph-macrophage infiltration with admixture consisting of numerous eosinophils and plasma cells. Paneth cells bunches were greatly visible in the base of intestinal epithelium crypts (Figure 5c). Solitary follicles were large and penetrated into submucous layer from proper layer. Peyer's plaques contained wide cell bunches of internodal lymphoid tissue. Crypts in Peyer's plaques view were not deep or they were even absent; villi were short and irregular-shaped. Lymphoid nodes formed mucous tunic evaginations between villi in a form of cupula covered with low prismatic epithelium with a great number of lymphocytes and macrophages. A moderate edema occurred in submucous layer; there was also diffuse lymph-macrophage infiltration with admixture consisting of numerous eosinophils. Muscular tunic in lymph follicles projection became substantially thinner.

Liver hepatocytes in animals from group 5 (silicon dioxide dose equal to 100 mg/kg of b.w.) had polygonal form, one or two nucleuses with fine-dispersed chromatin condensed at nuclear membrane and apparent nucleoluses. Hepatocytes cytoplasm was coarse-granular and eosinophilic (Figure 6a). Portal tract contained moderate infiltration from eosinophils, macrophages, and lymphocytes. Kupffer's cells were large and irregular-shaped; their prevalence was periportal. We observed feebly apparent mesangial cells proliferation in glomerules (up to 6 in a lobule) with a slight increase in mesangial matrix volume. There were no signs of proliferation of capsule external leaf cells (Figure 6b). Intraepithelial lymphoid tissue represented by solitary placed lymphocytes was greatly visible over a whole length of ileum mucous tunic epithelium. Villi had different width and form due to uneven edema and inflammatory infiltration consisting of macrophages, lymphocytes, and eosinophils (Figure 6c). Proper layer of mucous tunic contained a lot of macrophages, lymphocytes, plasma cells, and eosinophils.

Paneth cells bunches were well differentiated at the crypts bases. Solitary lymph nodes were large with big light prevailing reactive centers and wide cellular mantle zones; they penetrated into submucous layer from proper layer. Peyer's plaques contained up to 8 large secondary follicles and bunches of internodal lymphoid tissue and were located not only in proper layer but also in submucous layer. Crypts in Peyer's plaque projection were not deep or were not found at all; villi were short and irregular-shaped. Lymph nodes between villi evaginated mucous tunic into lumen in a form of a cupula covered with low epithelium (M-cells) with a big number of lymphocytes and macrophages. Follicles reactive centers contained centrocytes, centroblasts, immunoblasts, and a lot of macrophages. Mantle zones and internodal lymphoid tissue were represented by smaller lymphocytes with minute dark nucleuses, narrow cytoplasm ferrule, and macrophages. Submucous layer was represented by areolar fiber tissue with some lymphocytes bunches located in it, as well as with diffusely located eosinophils, macrophages, and plasma cells. Muscular tunic was substantially thinner in lymphatic follicles projection.

The obtained results reveal that there are changes in organs of animals from all the experimental groups in comparison with the control group. In case of liver, there is eosinophilic infiltration of portal tracts and granulosity of entherocytes cytoplasm; as for kidneys, we detected a relatively feebly apparent focal degeneration of nephron capsule external leaf. These changes don't have any evident dose-dependency in terms of introduced nanomaterial, and, as we may assume, they are quite similar to standard age-related changes which can occur in animals with age older than 4 months. Nevertheless, the trend which such changes have, in liver in particular, proves that there is a certain immune reaction enhancement caused by SiO_2 nanoparticles introduction.

Changes in ileum morphology are the most apparent; they include massive lymph-macrophage and eosinophilic infiltration of villi, submucous layer, and proper layer. The above-mentioned immune reaction enhance-

ment in ileum walls, which may result from SiO2 nanoparticles irritating effects, increases monotonically in the whole nanomaterial doses range. It doesn't allow us to determine the dose at which such changes authentically exceed the control group parameters. Still it is quite evident that when a maximum dose (100 mg/kg of body weight) is introduced, immune reaction enhancement in ileum wall becomes substantial.

Thus, amorphous SiO2 examined in this work is widely used in food industry as E551 food additive serving as anti-caking agent and a carrier. According to TR TS 029/012, E551 application is allowed in such food stuffs as spices (not more than 30 g/kg); products tightly wrapped in foil (30 g/kg); dry powder-like products including icing sugar (10 g/kg); cheese and its substitutes (10 g/kg); salt and its substitutes (10 g/kg); flavoring agents (50 g/kg). E551 is allowed to be used in children food products in a quantity up to 10 g/kg if this food additive is a part of a raw material which a finished product is made of. E551 application standard in such dry products as cereals made for children nutrition is 2 g/kg. E551 content is not regulated in biologically active additives to food and sugary confectionary (except chocolate) and is determined in accordance with a manufacturer's technical documentation. In most cases nano-sized structure of the applied silicon dioxide is not declared by food manufactures and it makes it next to impossible to define more or less precise volumes of this nanomaterial which are consumed with food.

As the experiment performed on mice [7] and dedicated to studying acute toxicity of nano-sized SiO2 showed, when the substance is once introduced via gastric tube in a dose equal to 10000 mg/kg, it doesn't lead to animals' death or intoxication. There were no morphologic changes in histological specimen of colon and jejunum.

On the other hand, according to research results obtained in experiments performed on a large number of model systems in vitro, SiO2 nanoparticles are cytotoxic when they contact with cells of various types. Thus, the work [15] describes how vitality of bronchial tubes epithelial cells (Beas-2B line) decreases due to the effects exerted by this nanomaterial; the material also causes peroxidation processes activation, shifts in proteom profile of intracellular kinase cascade enzymes. Increase in anti-inflammation cytokines production caused by amorphous SiO2 influence was detected in two lines of epithelial and endothelial cells in a lung [19]. Violation in nitrogen peroxide and peroxinitrite synthesis balance in vessels endothelium cells treated with these nanomaterials was detected in research [13] According to the results described in work [23], amorphous SiO2 nanoparticles in human cells of MCF-7 line were cytotoxic depending on a dose; they caused glutathione-S-transferase-1 hyperexpression in non-lethal concentrations. Thrombocytes aggregation effect was observed under SiO2 nanoparticles influence; the effect was mediated by influence exerted on balance between nitric oxide and peroxinitrite [14].

SiO2 nanoparticles caused damage to EAHY926 line cells, and here it should be noted that analog particles of sub-micron size (100-300nanometers) were not toxic [26]. Nano-sized SiO2 with particles diameter equal to 10 and 30, but not 80 nanometers suppressed differentiation into cardiac hystiocytes in stem cells culture of a mouse embryo [18]. Apoptosis and changes in p53, Bax and Bcl-2 expression caused by SiO2 nanoparticles with 21 nanometers size were detected in L-02 line hepatocytes [20]. Nanoparticles of such type led to release of multiple reactive oxygen forms, nitrogen oxide and TNF-□ in Kupffer's macrophages culture of rats' liver [12]. Research work [24] contains data on ability of the examined nanoparticles to stimulate autophagia processes in endothelial cells.

When amorphous SiO2 nanoparticles were introduced abdominally in very high doses (up to 2 g/kg of body weight), researchers detected shifts in peritoneal macrophages functions, higher production of IL-1b, TNF-a, NO, IL-1,6, TNF-agenes expression, nitrogen oxide synthase, and cyclooxigenase-2 [22]. Silica nanoparticles with diameter equal to 70 nanometers were hepatotoxic for rats when introduced intravenously in a dose equal to 30

mg/kg [21]. When nanomaterial was introduced into mice in the same manner in a dose 2-50 mg/kg of body weight, changes in CD3+, CD45+, CD4+ и CD8+ cells ratio in spleen were detected, and shifts in levels of crude immunoglobulins belonging to IgG and IgM classes occurred [28]. As per data taken from [29] SiO2 nanoparticles were able to enhance intranasal allergic sensitization of mice with an egg albumin model allergen. The same data on bronchial asthma model in rats caused by sensitization to an egg albumin were obtained in research work [17].

Authors in research work [27] examined subacute (during 84-day experiment) toxicity of two types of nanostructured SiO2 at oral introduction into rats in doses from 100 to 2500 mg/kg of body weight. An attempt to make quantitative assessment of SiO2 absorption and bioaccumulation in organs and tissues via mass-spectrometry led to ambiguous results due to high background level of silicon in organs of animals from control group. However, authentic increase in silicon content in liver and spleen of animals who received nanoparticles in the biggest doses was qualitatively fixed. Authors also detected dose-depending increase in fibrosis and expression of genes inducing this process in liver. Given all the above-mentioned parameters, authors assessed threshold dose (LOAEL) of SiO2 nanoparticles at subacute oral exposure as being equal to 2500 mg/kg of body weight, and maximum noneffective dose (NOAEL) was estimated to be equal to more than 100 mg/kg of body weight. The cited work has a drawback (and the authors themselves mention it) and it is related to very high doses of nanoparticles introduced into animals; such doses are incomparable to actual exposure with food which, according to authors' estimation, is equal to about 1.8 mg/kg of body weight a day. FSBSI Research Institute for Nutrition and FBSI Federal Scientific Center for Medical and Preventive Health Risk Management Technologies conducted joint research aimed at examining subacute oral toxicity which industrially manufactured nanostructured SiO2 of "Aerosil" type (with nanoparticles sized 20-60 nanometers) has for rats and mice; the experiment lasted for 92 days. As the results of research described in works [7–11] showed, animals which received SiO2 nanoparticles had apparent leucopenia, authentic decrease in T-helpers share and increase in cytotoxic lymphocytes share, immunoregulatory index (CD4/CD8) reduction, cytokines imbalance revealing itself in authentic multiple growth in TNF-alevel and apparent decrease in IL-10. Threshold dose of toxic effects exerted by SiO2nanoparticles at 92-day oral exposure for rats amounted to 100 mg/kg of body weight a day as per the examined parameters.

Morphologic data obtained in the current study confirm that if nano-sized SiO2 is introduced into animals' gastrointestinal tract under the same conditions, apparent immune reaction occurs in their ileum; this reaction extends onto lymphoid tissue associated with ileum wall and it becomes apparent in a form of massive lymph-macrophages and eosinophilic infiltration of villi without visible disorders in their epithelial layer structure. It can indirectly imply that there are no disorders in barrier function of intestinal epithelium and it coincides with the previously obtained results from work [8]. Given all the above-mentioned data on SiO2 nanoparticles research in systems in vitro and in vivo, we can assume that a trigger mechanism of such reaction is nanoparticles absorption by inter-epithelial macrophages and (or) macrophages contained in lymphatic follicles; it leads to further "respiratory blast" reaction, hyperproduction of reactive free-radical oxygen derivatives and production of anti-inflammatory cytokines and chemokines which cause involvement and activation of various immune cells. Such reaction can lead to systemic inflammation evolvement becoming apparent through above-mentioned shifts in T-cells immunity. At the same time, we need further examination (including ultrastructural level) if we want to get more information on details of local immune reaction evolvement in small intestine wall under exposure to SiO2 nanoparticles.

Conclusions. The examinations performed at light optical level detected evidence

of toxic effects exerted by SiO2 nanoparticles with specific surface area equal to 300 m2/g on animals' bodies at oral introduction in doses equal to 0.1-100 mg/kg of body weight during 92 days. First of all, these effects revealed themselves in immune and (or) inflammatory reaction evolvement in small intestine. The obtained results indicate there may be risks for human health when silicon dioxide (SiO2) with specific surface area equal to 300 m2/g and more is applied as a food additive in food industry.

References

1. Merkulov G.A. Kurs patologogistologicheskoj tehniki [Course of histopathologic technology]. Leningrad: Medicina, Leningradskoe otdelenie, 1969, 424 p. (in Russian).

2. Onishchenko G.G., Archakov A.I., Bessonov V.V., Bokit'ko B.G., Gincburg A.L., Gmoshinskij I.V., Grigor'ev A.I., Izmerov N.F., Kirpichnikov M.P., Narodickij B.S., Pokrovskij V.I., Potapov A.I., Rahmanin Ju.A., Tutel'jan V.A., Hotimchenko S.A., Shajtan K.V., Sheveleva S.A. Metodicheskie podhody k ocenke bezopasnosti nanomaterialov [Guidelines for evaluation of the safety of nanomaterials]. *Gigiena i sanitarija*, 2007, no. 6, pp. 3–10 (in Russian).

3. Mikroskopicheskaja tehnika: Rukovodstvo [Microscopic technique: Manual]. Ed.: D.S. Sarkisov, J.L. Petrov. Moscow, Medicina Publ., 1996, 544 p. (in Russian).

4. MU 1.2.2520–09. Toksikologo-gigienicheskaja ocenka bezopasnosti nanomaterialov: Metodicheskie ukazanija 1.2.2520–09 [Toxicological and hygienic evaluation of the safety of nanomaterials: Guidelines 1.2.2520–09]. Moscow, Federal'nyj centr gigieny i jepidemiologii Rospotrebnadzora, 2009, 35 p. (in Russian).

5. Ob utverzhdenii pravil laboratornoj praktiki: Prikaz Minzdravsocrazvitija Rossii № 708N ot 23.08.2010. [On approval of the rules of good laboratory practice: Order of the Health Ministry of Russia from 23.08.2010 № 708N]. Available at: http: //www.consultpharma.ru/index.php/ru/documents/drugs/299-708-23-2010 (10.10.2016) (in Russian).

6. Onishchenko G.G., Tutelyan V.A. O koncepcii toksikologicheskih issledovanij, metodologii ocenki riska, metodov identifikacii i kolichestvennogo opredelenija nanomaterialov [On concept of toxicological studies, methodology of risk assessment, metods of identification and quantity determining of nanomaterials]. *Voprosy pitanija*, 2007, vol. 76, no. 6, pp. 4–8 (in Russian).

7. Zaitseva N.V., Zemlyanova M.A., Zvezdin V.N., Dovbysh A.A., Gmoshinskiy I.V., Khotimchenko S.A., Safenkova I.V., Akafeva T.I. Toksikologicheskaja ocenka nanostrukturnogo dioksida kremnija. Parametry ostroj toksichnosti [Toxicological assessment of nanostructured silica. The acute oral toxicity]. *Voprosy pitanija*, 2014, vol. 83, no. 2, pp. 42–49 (in Russian).

8. Shumakova A.A., Arianova E.A., Shipelin V.A., Sidorova Ju.S., Selifanov A.V., Trushina Je.N., Mustafina O.K., Safenkova I.V., Gmoshinskij I.V., Hotimchenko S.A., Tutel'jan V.A. Toksikologicheskaja ocenka nanostrukturnogo dioksida kremnija. I. Integral'nye pokazateli, addukty DNK, uroven' tiolovyh soedinenij i apoptoz kletok pecheni [Toxicological assessment of nanostructured silica. I. Integral indices, adducts of DNA, tissue thiols and apoptosis in liver]. *Voprosy pitanija*, 2014, vol. 83, no. 3, pp. 52–62 (in Russian).

9. Shumakova A.A., Avren'eva L.I., Guseva G.V., Kravchenko L.V., Soto S.H., Vorozhko I.V., Sencova T.B., Gmoshinskiy I.V., Khotimchenko S.A., Tutelyan V.A. Toksikologicheskaja ocenka nanostrukturnogo dioksida kremnija II. Jenzimolo-gicheskie, biohimicheskie pokazateli, sostojanie sistemy antioksidantnoj zashhity [Toxicological assessment of nanostructured silica. II. Enzymatic, biochemical indices, state of antioxidative defence]. *Voprosy pitanija*, 2014, vol. 83, no. 4, pp. 58–66 (in Russian).

10. Shumakova A.A., Efimochkina N.R., Minaeva L.P., Bykova I.B., Batishheva S.Ju., Markova Ju.M., Trushina Je.N., Mustafina O.K., Sharanova N.Je., Gmoshinskij I.V., Hanfer'jan R.A., Khotimchenko S.A., Sheveleva S.A., Tutelyan V.A. Toksikologicheskaja ocenka nanostrukturnogo dioksida kremnija. III. Mikro-jekologicheskie, gematologicheskie pokazateli, sostojanie sistemy immuniteta [Toxicological assessment of nanostructured silica. III. Microecological, hematological indices, state of cellular immunity]. *Voprosy pitanija*, 2015, vol. 84, no. 4, pp. 55–65 (in Russian).

11. Shumakova A.A., Shipelin V.A., Trushina Je.N., Mustafina O.K., Gmoshinskiy I.V., Hanferyan R.A., Khotimchenko S.A., Tutelyan V.A. Toksikologicheskaja ocenka nanostrukturnogo dioksida kremnija. IV. Immuno-logicheskie i allergologicheskie pokazateli u zhivotnyh, sensibilizirovannyh pishhe-vym allergenom, i zakljuchitel'noe obsuzhdenie [Toxicological assessment of nanostructured silica. IV. Immunological and allergological indices in animals sensitized with food allergen and final discussioin]. *Voprosy pitanija*, 2015, vol. 84, no. 5, pp. 102–111 (in Russian).

12. Han B., Guo J., Abrahaley T. et al. Adverse Effect of Nano-Silicon Dioxide on Lung Function of Rats with or without Ovalbumin Immunization. *PLoS One*, 2011, vol. 6, no. 2, pp. e17236.

13. Corbalan J.J., Medina C., Jacoby A. et al. Amorphous silica nanoparticles aggregate human platelets: potential implications for vascular homeostasis. *Int. J. Nanomedicine*, 2012, vol. 7, pp. 631–639.

14. Corbalan J.J., Medina C., Jacoby A. [et al]. Amorphous silica nanoparticles trigger nitric oxide/peroxynitrite imbalance in human endothelial cells: inflammatory and cytotoxic effects. *Int. J. Nanomedicine*, 2011, vol. 6, pp. 2821–2835.

15. Chen Q., Xue Y., Sun J. Kupffer cell-mediated hepatic injury induced by silica nanoparticles in vitro and in vivo. *Int. J. Nanomedicine*, 2013, vol. 8, pp. 1129–1140.

16. Eom H.-J., Choi J. SiO2 Nanoparticles Induced Cytotoxicity by Oxidative Stress in Human Bronchial Epithelial Cell, Beas-2B. *Environ. Health Toxicol*, 2011, vol. 26, pp. e2011013.

17. Guide for the care and use of laboratory animals. Eighth Edition / Committee for the Update of the Guide for the Care and Use of Laboratory Animals; Institute for Laboratory Animal Research (ILAR); Division on Earth and Life Studies (DELS); National Research Council of the national academies. Washington: The National Academies Press, 2011, 246 p. Available at: https: //grants.nih.gov/grants/olaw/Guide-for-the-Care-and-use-of-laboratory-animals.pdf (10.10.2016).

18. Park M.V., Annema W., Salvati A., Lesniak A., Elsaesser A., Barnes C., McKerr G., Howard C.V., Lynch I., Dawson K.A., Piersma A.H., de Jong W.H. In vitro developmental toxicity test detects inhibition of stem cell differentiation by silica nanoparticles. *Toxicol. Appl. Pharmacol*, 2009, vol. 240, no. 1, pp. 108–116.

19. Kasper J., Hermanns M.I., Bantz C. et al. Inflammatory and cytotoxic responses of an alveolar-capillary coculture model to silica nanoparticles: Comparison with conventional monocultures. *Part. Fibre Toxicol*, 2011, vol. 8, pp. 6.

20. Shi J., Karlsson H.L., Johansson K. [et al.]. Microsomal glutathione transferase 1 protects against toxicity induced by silica nanoparticles but not by zinc oxide nanoparticles. *ACS Nano*, 2012, vol. 6, no. 3, pp. 1925–1938.

21. Ye Y., Liu J., Xu J., Sun L., Chen M., Lan M. Nano-SiO2 induces apoptosis via activation of p53 and Bax mediated by oxidative stress in human hepatic cell line. *Toxicol. In Vitro*, 2010, vol. 24, no. 3, pp. 751–758.

22. Park E.J., Park K. Oxidative stress and pro-inflammatory responses induced by silica nanoparticles in vivo and in vitro. *Toxicol. Lett*, 2009, vol. 184, no. 1, pp. 18–25.

23. Nishimori H., Kondoh M., Isoda K. [et al.]. Silica nanoparticles as hepa-totoxicants. *Eur. J. Pharm. Biopharm*, 2009, vol. 72, no. 3, pp. 496–501.

24. Duan J., Yu Yo., Yu Ya., Li Y., Huang P., Zhou X., Peng S., Sun Z. Silica nanoparticles enhance autophagic activity, disturb endothelial cell homeostasis and impair angiogenesis. *Part. Fibre Toxicol*, 2014, vol. 11, no. 1, pp. 50.

25. Silicon dioxide, amorphous. Rome: JECFA, 1973–1992, 2 p. Available at: http: //www.fao.org/fileadmin/user_upload/jecfa_additives/docs/Monograph1/Additive-385.pdf (10.10.2016).

26. Napierska D., Thomassen L.C., Rabolli V., Lison D., Gonzalez L., Kirsch-Volders M., Martens J.A., Hoet P.H. Size-dependent cytotoxicity of monodisperse silica nanoparticles in human endothelial cells. *Small*, 2009, vol. 5, no. 7, pp. 846–853.

27. Van der Zande M., Vandebriel R.J., Groot M.J., Kramer E., Rivera Z.E.H., Rasmussen K., Ossenkoppele J.S., Tromp P., Gremmer E.R., Peters R.J.B., Hendriksen P.J., Marvin H.J.P., Hoogenboom R.L.A.P., Peijnenburg A.A.M., Bouwmeester H. Sub-chronic toxicity study in rats orally exposed to nanostructured silica. *Part. Fibre Toxicol*, 2014, vol. 11, pp. 8.

28. Lee S., Kim M.-S., Lee D., Kwon T.K., Khang D., Yun H.-S., Kim S.-H. The comparative immunotoxicity of mesoporous silica nanoparticles and colloidal silica nanoparticles in mice. *Int. J. Nanomedicine*, 2013, vol. 8, pp. 147–158.

29. Yoshida T., Yoshioka Y., Fujimura M. [et al]. Promotion of allergic immune responses by intranasally-administrated nanosilica particles in mice. *Nanoscale Res. Lett*, 2011, vol. 6, no. 1, pp. 192–204.

Zaitseva N.V., Zemlyanova M.A., Zvezdin V.N., Dovbysh A.A., Gmoshinskiy I.V., Khotimchenko S.A. Impact of silica dioxide nanoparticles on the morphology of internal organs in rats by oral supplementation. Health Risk Analysis, 2016, no. 4, pp. 74–87. DOI: 10.21668/health.risk/2016.4.10.eng

Received: 18.09.2016
Accepted: 30.11.2016
Published: 30.12.2016